P,N Ligands

Quadruple Deprotonation of 2-Aminophenylphosphane with a p-Block-Metal/Alkali-Metal Base**

Felipe García, Simon M. Humphrey, Richard A. Kowenicki, Eric J. L. McInnes, Christopher M. Pask, Mary McPartlin, Jeremy M. Rawson, Matthew L. Stead, Anthony D. Woods, and Dominic S. Wright**

The application of superbases, such as the well-known Schlosser base consisting of *t*BuOK and RLi, in the deprotonation of organic substrates is well established.[1] Recently, Mulvey investigated the structural chemistry and applications of related mixed-metal amide reagents.[2] These species show remarkable activity and specificity in their reactions with aromatic hydrocarbons and ferrocene (Cp_2Fe; Cp = cyclopentadienyl).[3,4] For example, the treatment of Cp_2Fe with a mixture of $i\mathrm{Pr}_2\mathrm{NH}/\mathrm{Bu}_2\mathrm{Mg}$ and *n*BuNa results in a double 1,3-deprotonation of the two Cp rings.[3] We recently observed that the stepwise reaction of MesPH_2 (Mes = 2,4,6-$\mathrm{Me}_3\mathrm{C}_6\mathrm{H}_2$) with BnNa (Bn = benzyl) and $[\mathrm{Sn(NMe}_2)_2]$ results in the unusual stannate ion $[\mathrm{Sn}(2\text{-}\mathrm{CH}_2\text{-}4,6\text{-}\mathrm{Me}_2\mathrm{C}_6\mathrm{H}_2)(\mathrm{PMes})]^{3-}$, which arises from the intermolecular deprotonation of a methyl group (Scheme 1).[5] We wanted to examine the activity of this type of p-block-metal/alkali metal reaction system further because this $\mathrm{Sn^{II}}$/BnNa system effectively acts as a superbase and there is a close relationship between this C–H activation reaction and activation reactions mediated by transition metals.[6] Herein, we present the observation that the reaction of 2-aminophenylphosphane (1-PH_2-2-$\mathrm{NH}_2\mathrm{C}_6\mathrm{H}_4$) with *n*BuLi (1 equiv) followed by the addition of $[\mathrm{Sn(NMe}_2)_2]$ (1 equiv) results in remarkable quadruple deprotonation of the ligand (Scheme 2) and generates the unusual paramagnetic $\mathrm{Sn^{II}}$-centered cage $[\{[\mathrm{Sn(L)(NMe_2)Li(thf)}][\mathrm{Sn(L)Li(thf)_3}]\mathrm{Sn}\}_2]$ (**1**) containing L^{4-} and $L^{3-\cdot}$ ions (L = ligand; see the Experimental Section).

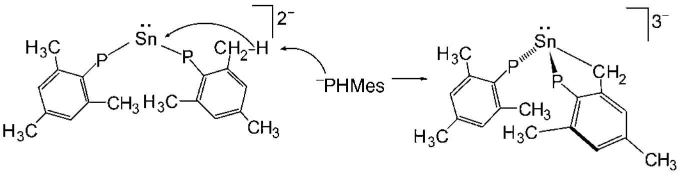

Scheme 1. Formation of $[\mathrm{Sn}(2\text{-}\mathrm{CH}_2\text{-}4,6\text{-}\mathrm{Me}_2\mathrm{C}_6\mathrm{H}_2)(\mathrm{PMes})]^{3-}$ through intermolecular *ortho* deprotonation of a C–H bond.

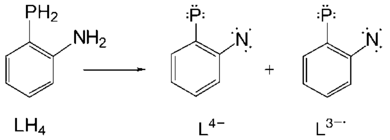

Scheme 2. The deprotonation of LH_4 by $[\mathrm{Sn(NMe}_2)_2]$/*n*BuLi. LH_4 = 1-PH_2-2-$\mathrm{NH}_2\mathrm{C}_6\mathrm{H}_4$, L = ligand.

No N–H or P–H stretching bands are found in the IR spectrum of solid **1**, thus showing that the NH_2 and PH_2 groups of the ligand have been completely deprotonated. As far as we can gauge, neither $[\mathrm{Sn(NMe}_2)_2]$ nor *n*BuLi alone will cause deprotonation to this extent. The surprising paramagnetic character of **1** was indicated initially by ^{1}H and ^{31}P NMR spectroscopic studies: only a broad resonance in the aromatic region appears in the ^{1}H NMR spectrum at room temperature, and a very broad singlet appears at approximately $\delta = 10$–15 ppm in the $^{31}\mathrm{P}\{^1\mathrm{H}\}$ NMR spectrum. Compound **1** in the solid state exhibits a strong signal in the EPR spectrum at both the X and K bands (Figure 1). The spectral width is identical at both frequencies, which means that this signal can not be interpreted as a rhombic set of *g* values. Therefore, we attempted to simulate the spectra on the basis of 1) hyperfine coupling in which the two unpaired electrons are independent of each other and 2) hyperfine coupling with an exchange interaction (a biradical system). It was not possible to reproduce the relative intensities of the transitions by assuming coupling to ^{31}P or ^{117,119}Sn nuclei[7] for any set of parameters that were tried (including the number of nuclei), nor was it possible to simulate the spectra on the basis of a biradical system with coupling to these isotopes or the

---

[*] F. García, S. M. Humphrey, R. A. Kowenicki, Dr. C. M. Pask,
Dr. J. M. Rawson, M. L. Stead, Dr. A. D. Woods, Dr. D. S. Wright
Chemistry Department
University of Cambridge
Lensfield Road, Cambridge CB21EW (UK)
Fax: (+44) 1223-336-362
E-mail: dsw1000@cus.cam.ac.uk

Dr. E. J. L. McInnes
The EPSRC cw EPR Service Centre
University of Manchester
Oxford Road, Manchester M139PL (UK)

Prof. M. McPartlin
Department of Health and Human Sciences
London Metropolitan University
Holloway Road, London N78DB (UK)

[**] We thank the EPSRC (S.M.H., C.M.P., M.M., J.M.R., and D.S.W); St. Catharine's College, Cambridge (fellowship for A.D.W.); The Cambridge European Trust and Newton Trust (F.G.); the States of Guernsey; and The Domestic and Millennium Fund (R.A.K.) for financial support. Acknowledgment is made to the donors of the American Chemical Society Petroleum Research Fund for partial support of this research (M.L.S.). We also thank Dr. J. E. Davies (Cambridge) for collecting X-ray data for compound **1**.

DOI: 10.1002/ange.200500340

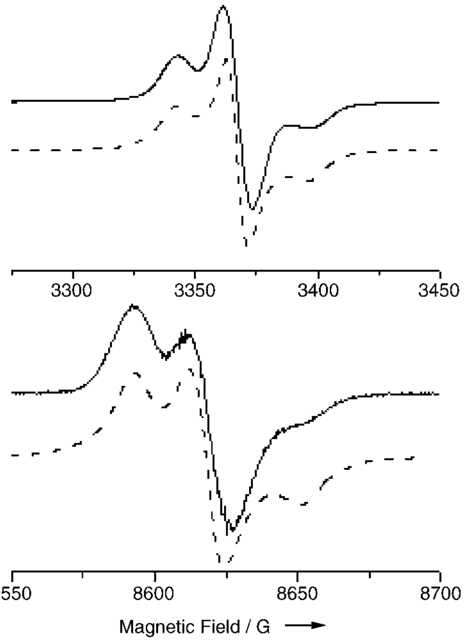

Figure 1. Experimental (solid lines) and simulated (from parameters in the text; dashed lines) EPR spectra of a powdered sample of **1** at 295 K; top: at the X band (9.448 GHz) and bottom: at the K band (24.167 GHz).

^{14}N isotope. The only good simulations were obtained by assuming coupling of each unpaired electron to a single ^{14}N nucleus (with no interaction between the two unpaired electrons) with the parameters $g_{x,y} = 2.004$, $g_z = 2.002$, $A_z = 27 \times 10^{-4}\,\text{cm}^{-1}$, and $A_{x,y}$ held at an arbitrarily small value of $1\text{x}10^{-4}\,\text{cm}^{-1}$. The $A_z(^{14}\text{N})$ value places an upper limit of approximately 45 % on the unpaired electron density in the 2p orbital of the N atom. The lack of resolution of the ^{31}P nuclei coupling in the EPR spectrum suggests that this coupling constant is smaller than the experimentally obtained linewidths (ca. 10 G).

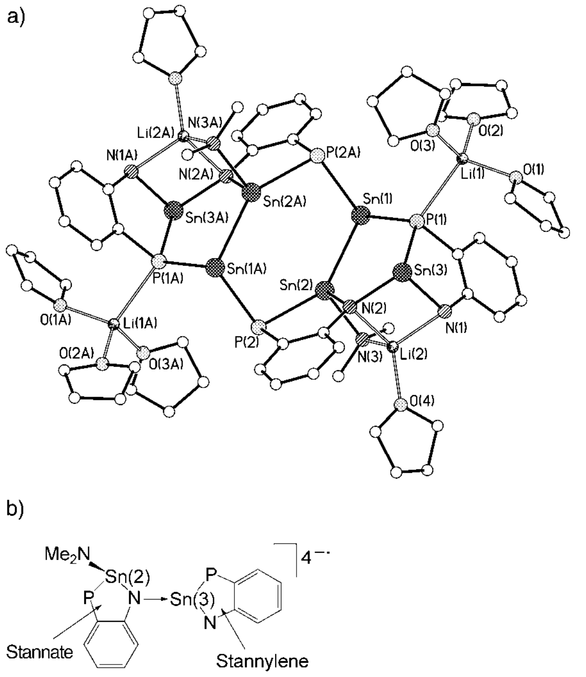

Figure 2. a) Molecular structure of **1**. Hydrogen atoms and lattice-bound THF molecules have been omitted for clarity; disorder of the THF molecules is not shown. Selected bond lengths [Å] and angles [°]: Sn(1)–P(1) 2.603(4), Sn(1)–P(2A) 2.607(4), Sn(1)–Sn(2) 2.885(1), Sn(2)–N(2) 2.10(1), Sn(2)–N(3) 2.18(1), Sn(3)–N(1) 2.18(1), Sn(3)–N(2) 2.17(1), Sn(3)–P(1) 2.566(4), Li(1)–P(1) 2.56(3), Li(2)–N 2.00(3)–2.14(3); angles about Sn(1): 86.21(9)–103.58(9), Sn(2): 88.4(3)–145.9(1), Sn(3): 81.0(3)–99.7(3). b) Schematic representation of the stannate/stannylene $[\text{Sn}_2(\text{L})_2(\text{NMe}_2)]^{4-\cdot}$ ion of **1**.

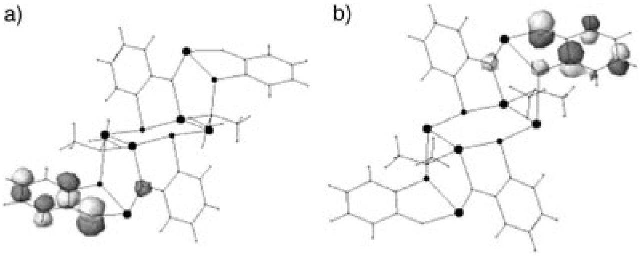

Figure 3. Representation of the semiempirical component PM5-derived frontier MOs of **1**, which illustrates their ligand-based π character: a) the HOMO and b) the LUMO. Large spheres = Sn atoms, small spheres = P atoms.

The low-temperature X-ray crystal structural analysis of **1**[8] (combined with the previous spectroscopic data) shows that the complex consists of centrosymmetric molecules with the formula $[\{[\text{Sn}(\text{L})(\text{NMe}_2)\text{Li}(\text{thf})][\text{Sn}(\text{L})\text{Li}(\text{thf})_3]\text{Sn}\}_2]$ (Figure 2 a). Consistent with the main conclusion drawn from the EPR studies, semiempirical calculations on the $[\text{Sn}_6(\text{L})_4(\text{NMe}_2)_2]^{4-\cdot}$ ion of **1** (see Figure 3, in which the tris-THF-solvated Li$^+$ ions and the THF solvation have been omitted) show that the frontier orbitals are ligand based (85 %) rather than Sn based.[9] Furthermore, the majority of the spin density is found on the nitrogen centers of the ligands located at the periphery of the cage (as indicated in Figure 3). The calculated spin density of 30 % on the nitrogen centers of these ligands is in good agreement with the upper estimate of 45 % based on EPR studies. Interestingly, the spin densities on the nitrogen and phosphorus centers of the ligands within the central portion of the molecule are an order of magnitude less (no greater than 5 %). This distribution explains why the complex behaves as a biradical, in which there is no interaction between the unpaired electrons. The major deduction drawn from the spectroscopic and molecular orbital (MO) studies is that to attain electronic neutrality the hexanuclear Sn$_6$ arrangement of **1** must consist of six Sn$^{\text{II}}$ centers together with two tetraanions L^{4-} and two radical trianions L$^{3-\cdot}$, as well as two NMe$_2$ groups, rather than the potential metal-centered alternative consisting of two Sn$^{\text{III}}$ and four Sn$^{\text{II}}$ ions and four L^{4-} ions.

The biradical arrangement of **1** consists of two symmetry-related stannylene/stannate fragments (Figure 2 b) that are connected by two Sn$^{\text{II}}$ centers within the central $(\text{Sn}_2\text{P})_2$ ring of **1** through Sn–Sn and Sn–P bonds. The Sn–Sn bonds within the $(\text{Sn}_2\text{P})_2$ ring (Sn(2)–Sn(1) = 2.885(1) Å) are best described as dative bonds between eight-electron stannate (donor) and Sn^{II} centers (acceptor). These bonds are considerably shorter than the dative Sn−Sn bonds in [ArSn^{II}→Sn^{II}\{1,8-(NR)$_2$C$_{10}$H$_6$\}] (Ar = 2,6-(Me$_2$N)$_2$C$_6$H$_3$; Sn−Sn = 3.087(2) Å),[10] but similar in length to the bonds in the most closely related species [(Me$_3$Si)$_3$Sn^{II}→Sn^{II}\{2-[(Me$_3$Si)$_2$C]C$_5$H$_4$N\}] (Sn−Sn = 2.8689(5) Å).[11] The Sn−P and Sn−N bond lengths (2.497(4)–2.607(4) and 2.10(1)–2.18(1) Å, respectively) are within the range observed for structurally characterized Sn^{II}−P and Sn^{II}−N compounds.[12] The shortest of the Sn−P and Sn−N bond lengths in **1** are in the \{Sn(N−C$\overset{\cdots}{-}$C−P)\} chelate rings, with Sn(1)−P bonds (mean = 2.605(4) Å) being the longest bonds of this type in the structure. This Sn(1) centre has a highly distorted pyramidal geometry (range of angles about Sn(1) = 86.21(9)–103.58(9)°), which is similar to that found at the stannylene center Sn(3) (range = 81.0(3)–99.7(3)°). The neutrality of the molecular arrangement of **1** is completed by four Li$^+$ ions that are located at the periphery of the cage. The Li(1)(thf)$_3$ center is bonded to a P atom (Li(1)−P(1) = 2.56(3) Å), and the Li(2)(thf) center is coordinated by three N centers of the core (Li(2)−N = 2.00(3)–2.14(3) Å).

Although symmetrical N-heterocyclic germylenes,[13] silylenes,[14] and stannylenes[15] have been studied extensively in the past decade, and noncyclic N−Sn−O and N−Sn−C stannylenes are known,[16,17] the N,P-stannylene arrangement found in **1** is unique for a heterocyclic species. To the best of our knowledge, the extent of the deprotonation observed in this study is without precedent for a simple organic acid when treated with a base in solution. The deprotonation of both the NH$_2$ and PH$_2$ groups of 2-aminophenylphosphane is particularly dramatic bearing in mind the large negative charge that develops in the resulting L^{4-} and L$^{3-\cdot}$ ions. The results reported herein show that multiple deprotonation of organic acids by mixed alkali-metal organometallic/p-block-metal dimethylamide reagents is a promising area for future study.

Experimental Section

*n*BuLi (3.1 mL, 1.6 mol L^{-1} in hexanes, 5.0 mmol) was added to 2-aminophenylphosphane (0.47 mL, 5.0 mmol) in THF (20 mL) was carried out at −78 °C. The reaction mixture was warmed to room temperature and stirred for 4 h to yield a red solution. The reaction mixture was then cooled to −78 °C, and [Sn(NMe$_2$)$_2$] (1.10 g, 5.0 mmol) was added as a solution in THF (10 mL). The reaction mixture was warmed to room temperature and stirred for 16 h to yield a dark-red solution. The solvent was reduced in volume to 5–10 mL and filtered. Complex **1** (0.20 g, 10 % yield based on Sn) was crystallized from the filtrate at −30 °C (ca. 1 week). IR (nujol): $\tilde{\nu}$ = 1583 (m), 1020 (s), 816 (m), 765 (w), 735 cm^{-1} (m); ^{1}H NMR (25 °C, 500.16 MHz, [D$_8$]THF): δ = 7.5–5.7 (collection of overlapping multiplets), 3.50 (m, -CH$_2$-, THF), 1.70 ppm (m, -CH$_2$-O, THF) the aromatic resonances were not resolved when the temperature was lowered to −80 °C; ^{31}P NMR (25 °C, 161.975 MHz, [D$_8$]THF, reference: 85 % H$_3$PO$_4$/D$_2$O): δ = 10–15 ppm (v br s); elemental analysis (%) calcd for C$_{64}$H$_{100}$Li$_4$N$_6$O$_9$P$_4$Sn$_6$: C 37.7, H 4.8, N 4.4, P 5.9; found C 39.2, H 5.1, N 4.3, P 6.3. The X-ray crystallographic analysis of **1** was carried out on batches of crystals from two separate reactions to confirm the reproducibility and consistency of the product obtained. Although the yield of **1** is low, the paramagnetic nature of the other products of this reaction that are present in solution made it impossible to obtain further NMR spectroscopic data on them (through, the absence of crystalline material). However, other products may well be expected if one bears in mind that the 1:1:1 reaction stoichiometry of *n*BuLi/[Sn(NMe$_2$)$_2$]/LH$_4$ is different from the observed stoichiometry of the components in **1**.

Received: January 28, 2005
Published online: April 28, 2005

Keywords: deprotonation · lithium · metal–metal bonding · tin · X-ray diffraction

---

[1] L. Lochmann, *Eur. J. Inorg. Chem.* **2000**, *39*, 115.
[2] R. E. Mulvey, *Chem. Commun.* **2001**, 1049.
[3] D. R. Armstrong, A. R. Kennedy, R. E. Mulvey, R. B. Rowlings, *Angew. Chem.* **1999**, *111*, 231; *Angew. Chem. Int. Ed.* **1999**, *38*, 131.
[4] W. Clegg, K. W. Henderson, A. R. Kennedy, R. E. Mulvey, C. T. O'Hara, R. B. Rowlings, D. M. Tooke, *Angew. Chem.* **2001**, *113*, 4020; *Angew. Chem. Int. Ed.* **2001**, *40*, 3902.
[5] M. McPartlin, A. D. Woods, C. M. Pask, T. Vogler, D. S. Wright, *Chem. Commun.* **2003**, 1524.
[6] Z. Hou, D. W. Stephan, *J. Am. Chem. Soc.* **1992**, *114*, 10088; Z. Hou, T. L. Breen, D. W. Stephan, *Organometallics* **1993**, *12*, 3158.
[7] Although the observed g value is within the range previously observed for Sn-centred radicals (g = 1.988–2.077) there is no evidence for hyperfine coupling to the Sn nuclei; previously reported coupling constants (a(^{117,119}Sn) = 329–3426 G) are much greater than the linewidth of 10–15 G observed in the spectrum of **1**; J. Iley, *The Chemistry of Organic Germanium, Tin and Lead* (Ed.: S. Patai), Wiley, New York, **1993**, chap. 5; A. Sekiguchi, T. Fukawa, V. Y. Lee, M. Nakamoto, *J. Am. Chem. Soc.* **2003**, *125*, 9250.
[8] Crystal data for **1**: C$_{64}$H$_{100}$Li$_4$N$_6$O$_9$P$_4$Sn$_6$, M_r = 1961.28, monoclinic, space group *C*2/*c*, Z = 4, a = 33.0513(16), b = 17.4337(7), c = 16.6854(9) Å, β = 98.209(2)°, V = 9515.7(8) Å^3, μ(Mo$_{K\alpha}$) = 1.661 mm^{-1}, ρ_{calcd} = 1.370 Mg m^{-3}, T = 180(2) K. Data were collected on a Nonius KappaCCD diffractometer. Of a total of 14976 reflections collected, 4813 were unique (R_{int} = 0.151). The structure was solved by direct methods and refined by full-matrix least-squares on F^2 (G. M. Sheldrick, *SHELX-97*, Göttingen, Germany, **1997**). Final $R1$ = 0.079 ($I > 2\sigma(I)$) and $wR2$ = 0.213 (all data). CCDC-261960 contains the supplementary crystallographic data for this paper. These data can be obtained free of charge from the Cambridge Crystallographic Data Centre via www.ccdc.cam.ac.uk/data_request/cif.
[9] Single-point semiempirical calculations were performed by using MOPAC implemented through the quantum cache version 5.0 (Fujitsu). PM5 parameters were employed on the assumption of an RHF state (neglecting electron–electron correlation). This process yielded a near-degenerate pair of singly occupied MOs with an energy separation of 0.056 eV (5.4 kJ mol^{-1}). These MOs comprise the in-phase and out-of-phase combinations ($\sqrt{2}$-($\Phi_a \pm \Phi_b$)) of the frontier MOs depicted in Figure 3, which were calculated from a closed-shell configuration. Further SCF calculations confirmed that the structure is a minimum on the potential-energy surface.
[10] C. Drost, P. B. Hitchcock, M. F. Lappert, *Angew. Chem.* **1999**, *111*, 1185; *Angew. Chem. Int. Ed.* **1999**, *38*, 1113.
[11] C. J. Cardin, D. J. Cardin, S. P. Constantine, A. K. Todd, S. J. Teat, S. Coles, *Organometallics* **1998**, *17*, 2144.
[12] Conquest Software for searching the Cambridge Structural Database and visualizing crystal structures: I. J. Bruno, J. C. Cole, P. R. Edgington, M. Kessler, C. F. Macrae, P. McCabe, J. Pearson, R. Taylor, *Acta Crystallogr. Sect. B* **2002**, *58*, 389.
[13] M. Denk, R. Lennon, R. Hayashi, R. West, A. V. Belyakov, H. P. Verne, A. Haaland, M. Wagner, N. Metzier, *J. Am. Chem. Soc.*

1994, *116*, 2691; B. Gerrhus, M. F. Lappert, J. Heinicke, R. Boese, D. Blaser, *J. Chem. Soc. Chem. Commun.* **1995**, 1931; B. Gerrhus, M. F. Lappert, J. Heinicke, R. Boese, D. Blaser, *J. Organomet. Chem.* **1996**, *521*, 211; D. F. Moser, I. A. Guzei, R. West, *Main Group Met. Chem.* **2001**, *24*, 811.

[14] J. Pfeiffer, W. Maringgele, M. Noltemeyer, A. Meler, *Chem. Ber.* **1989**, *122*, 245; W. Hermann, M. Denk, J. Behm, W. Scherer, F.-R. Klingan, H. Bock, B. Solouki, M. Wagner, *Angew. Chem.* **1992**, *104*, 1489; *Angew. Chem. Int. Ed. Engl.* **1992**, *31*, 1485; O. Kuhl, P. Lonnecke, J. Heinicke, *Polyhedron* **2001**, *20*, 221.

[15] a) H. Braunschweig, B. Gerrhus, P. B. Hitchcock, M. F. Lappert, *Z. Anorg. Allg. Chem.* **1995**, *621*, 1922; b) F. E. Hahn, L. Wittenbecher, M. Kuhl, T. Lugger, R. Frohlich, *J. Organomet. Chem.* **2001**, *617*, 629; c) T. Gans-Eichler, D. Gudat, M. Nieger, *Angew. Chem.* **2002**, *114*, 1966; *Angew. Chem. Int. Ed.* **2002**, *41*, 1888.

[16] L. Pu, M. M. Olmstead, P. P. Power, *Organometallics* **1998**, *17*, 5602; H. Braunschweig, R. W. Chorley, P. B. Hitchcock, M. F. Lappert, *J. Chem. Soc. Chem. Commun.* **1992**, 1311.

[17] See also: M. Driess, R. Janoschek, H. Pritzkow, U. Winkler, *Angew. Chem.* **1995**, *107*, 1746; *Angew. Chem. Int. Ed. Engl.* **1995**, *34*, 1614.